THE ASTROPHYSICAL JOURNAL, 312:254–270, 1987 January 1

THE BAADE-WESSELINK METHOD AND THE DISTANCES TO RR LYRAE STARS. II. THE FIELD STAR X ARIETIS

RODNEY V. JONES[1] AND BRUCE W. CARNEY[1]
University of North Carolina

AND

DAVID W. LATHAM AND ROBERT L. KURUCZ
Harvard-Smithsonian Center for Astrophysics
Received 1986 May 7; accepted 1986 June 25

ABSTRACT

We have obtained new VR and JHK photometry and radial velocities with typical accuracies of 1 km s^{-1} for the metal-poor RR Lyrae field star X Arietis. We have utilized these data, along with unpublished *uvby* photometry of M. Siegel, to derive the distance to X Ari using two variations of the Baade-Wesselink method. We investigate the possibility of photospheric velocity gradients that might distort the value of the systemic velocity and cause a phase shift, and conclude that no gradient exists in the part of the stellar atmosphere considered here. The phasing problem previously noted for VY Ser by Carney and Latham (1984) also occurs for X Ari when optical photometry is used to compute the effective temperatures but not when the $V-K$ color index is used. We discuss possible causes of these phase shifts, and conclude that X Ari has $\langle M_V \rangle = 0.88 \pm 0.15$ mag on the basis of the $V-K$ results.

Subject headings: stars: individual — stars: luminosities — stars: pulsation — stars: RR Lyrae

I. INTRODUCTION

Knowledge of the absolute brightness of RR Lyrae variable stars is critical because they are used to measure the distances to the Galactic center (Oort and Plaut 1975), globular clusters (cf. Sandage 1982), and the nearer galaxies (Graham 1973, 1975, 1977; van den Bergh and Pritchet 1986). The distances to globular clusters are necessary to determine their ages accurately (Sandage 1982). However, there is as yet no agreement as to whether or not all RR Lyrae stars possess the same luminosity, since this quantity should depend on the star's composition and its history of mass loss during the preceding red giant phase.

There are four different methods employed to estimate the value of $\langle M_V \rangle_{RR}$: (1) statistical parallax of field variables (Hemenway 1975; Heck and Lakaye 1978; Clube and Dawe 1978, 1980; Hawley *et al.* 1986; Strugnell, Reid, and Murray 1986), (2) main-sequence fitting of globular clusters with field halo dwarfs with reliable trigonometric parallaxes (Sandage 1970; Carney 1980), (3) observations of RR Lyrae stars in the Magellanic Clouds, whose distances are determined by other means (Graham 1973, 1975, 1977), and (4) Baade-Wesselink analysis of field variables (Woolley and Savage 1971; Woolley and Dean 1976; McNamara and Feltz 1977; McDonald 1977; Wallerstein and Brugel 1979; Manduca *et al.* 1981; Siegel 1980, 1982; Longmore *et al.* 1985; Burki and Meylan 1986*a*, *b*). As will be discussed later, these methods yield results that are in sharp disagreement with each other. A value of $\langle M_V \rangle = 0.6 \pm 0.2$ mag is often assumed; however, this value is open to question.

Of these four methods, only the Baade-Wesselink type of analysis can measure the distances of these stars directly. This is important for the cluster stars because they may have undergone a different chemical history than the field stars (Kraft *et al.* 1982; Kraft 1982), and thus a method based on field stars may not be valid for them. The main drawback to the application of the Baade-Wesselink method in the past was the scarcity of accurate radial velocity curves. However, with the implementation of spectrometers such as the digital speedometer on the Multiple Mirror Telescope (MMT) (Latham 1985; Wyatt 1985), this drawback is being overcome. An attempt was made to apply two variations of this method to the field star VY Ser (Carney and Latham 1984, hereafter CL), but no value of $\langle M_V \rangle$ was obtained, owing to an unforeseen phasing problem despite the use of simultaneous photometry and spectroscopy. Since CL suggested that a possible source of this problem is that VY Ser may be cool enough that subsurface convection may distort the colors and hence the temperatures they derived, we have undertaken a similar study of the hotter variable X Ari.

Another possible source of the phasing error is the uncertainty in the stellar systemic velocity, γ. As discussed by Oke, Giver, and Searle (1962, hereafter OGS), if the spectral lines used to derive radial velocities form at differing mass depths at different phases, integration over the radial velocity cycle could yield an incorrect value for γ and would then introduce a phasing problem (see § III*b* and eq. [5] below). We have investigated this problem by measuring radial velocities in X Ari for individual lines that form in a wide range of mass depths.

II. OBSERVATIONS

a) Photometry

During three nights in 1982 December and four nights in 1983 October, we obtained VR_C photometry for X Ari using the KPNO No. 2 0.9 m telescope. All the nights were photometric. Extinction was measured each night, as were 15–20 standards from Landolt (1983). Two comparison stars near X Ari were observed frequently to monitor the transparency and incidentally set up local standards in case of future weather

[1] Visiting Astronomer, Kitt Peak National Observatory, which is operated by the Association of Universities for Research in Astronomy, Inc., under contract with the National Science Foundation.

TABLE 1

VR_C PHOTOMETRY

HJD (-2445000)	Phase	V	$V-R_C$	HJD (-2445000)	Phase	V	$V-R_C$
309.8512	0.6513	9.831	0.389	635.8712	0.3299	9.591	0.361
309.8597	0.6644	9.831	0.385	635.8820	0.3464	9.619	0.368
309.8705	0.6807	9.829	0.390	635.8961	0.3680	9.644	0.369
309.8741	0.6863	9.825	0.391	635.9067	0.3845	9.667	0.382
309.8784	0.6930	9.821	0.394	635.9205	0.4055	9.698	0.382
309.8826	0.6994	9.811	0.385	635.9373	0.4314	9.730	0.385
309.8868	0.7059	9.086	0.381	635.9524	0.4551	9.750	0.388
309.8909	0.7121	9.797	0.385	636.7123	0.6221	9.849	0.391
309.8943	0.7175	9.799	0.382	636.7194	0.6330	9.839	0.391
310.6149	0.8242	9.931	0.379	636.7208	0.6351	9.834	0.387
310.6182	0.8292	9.935	0.380	636.7299	0.6487	9.846	0.393
310.6218	0.8345	9.937	0.381	636.7311	0.6506	9.845	0.392
310.6626	0.8971	9.800	0.357	636.7468	0.6746	9.841	0.388
310.6660	0.9023	9.753	0.353	636.7480	0.6764	9.840	0.393
310.6697	0.9081	9.691	0.343	636.7623	0.6985	9.827	0.390
310.6708	0.9098	9.668	0.335	636.7635	0.7003	9.819	0.387
310.6732	0.9134	9.629	0.323	636.7740	0.7163	9.820	0.379
310.6743	0.9151	9.625	0.319	636.7752	0.7182	9.802	0.381
310.6758	0.9173	9.620	0.316	636.7832	0.7305	9.800	0.375
310.6768	0.9189	9.592	0.304	636.7842	0.7320	9.797	0.374
310.6777	0.9204	9.542	0.298	636.7968	0.7514	9.821	0.377
310.6787	0.9219	9.478	0.300	636.7980	0.7532	9.819	0.372
310.6799	0.9237	9.438	0.296	636.8132	0.7765	9.950	0.387
310.6810	0.9254	9.406	0.291	636.8144	0.7784	9.951	0.376
310.6825	0.9277	9.383	0.286	636.8199	0.7869	9.919	0.388
310.6835	0.9293	9.381	0.281	636.8211	0.7887	9.891	0.381
310.6858	0.9327	9.375	0.270	636.8228	0.7913	9.893	0.378
310.6895	0.9384	9.313	0.267	636.8363	0.8121	9.925	0.383
310.6905	0.9399	9.294	0.263	636.8373	0.8139	9.926	0.383
310.6915	0.9415	9.283	0.262	637.8316	0.3410	9.621	0.371
310.6926	0.9433	9.268	0.259	637.8349	0.3461	9.616	0.367
310.6937	0.9448	9.248	0.254	637.8385	0.3513	9.628	0.370
310.6946	0.9463	9.232	0.251	637.8429	0.3582	9.637	0.370
310.6956	0.9479	9.220	0.246	637.8474	0.3650	9.647	0.370
310.6967	0.9495	9.201	0.246	637.8577	0.3808	9.667	0.372
310.7004	0.9552	9.136	0.232	637.8611	0.3860	9.676	0.378
310.7014	0.9567	9.118	0.228	637.8770	0.4104	9.711	0.381
310.7024	0.9582	9.104	0.225	637.8801	0.4153	9.712	0.384
310.7034	0.9598	9.094	0.226	637.9036	0.4514	9.756	0.391
310.7044	0.9613	9.079	0.222	637.9166	0.4560	9.756	0.390
310.7057	0.9633	9.067	0.218	637.9195	0.4757	9.776	0.393
310.7064	0.9643	9.059	0.219	637.9355	0.5003	9.796	0.392
310.7026	0.9663	9.048	0.216	637.9369	0.5024	9.794	0.394
310.7097	0.9695	9.034	0.211	637.9544	0.5294	9.811	0.399
310.7107	0.9710	9.042	0.214	637.9573	0.5340	9.806	0.391
310.7117	0.9725	9.035	0.207	639.6985	0.2081	9.432	0.320
310.7127	0.9741	9.024	0.207	639.7023	0.2139	9.441	0.321
310.7137	0.9756	9.010	0.209	639.7057	0.2189	9.446	0.324
310.7147	0.9772	8.999	0.209	639.7155	0.2340	9.478	0.331
310.7157	0.9787	8.988	0.206	639.7187	0.2388	9.479	0.331
310.7167	0.9802	8.985	0.205	639.7220	0.2440	9.487	0.334
310.7179	0.9821	8.981	0.206	639.7351	0.2641	9.514	0.340
310.7199	0.9851	8.975	0.206	639.7382	0.2689	9.522	0.344
310.8042	0.1145	9.257	0.274	639.7415	0.2738	9.530	0.343
310.8083	0.1209	9.278	0.277	639.7538	0.2928	9.553	0.349
310.8118	0.1262	9.286	0.282	639.7569	0.2975	9.556	0.351
310.8158	0.1324	9.292	0.278	639.7602	0.3026	9.566	0.354
310.8418	0.1724	9.364	0.305	639.7749	0.3252	9.601	0.363
310.8451	0.1777	9.373	0.304	639.7780	0.3300	9.610	0.365
315.8265	0.8278	9.931	0.383	639.7814	0.3352	9.618	0.368
315.8351	0.8405	9.936	0.380	639.8023	0.3673	9.646	0.374
315.8384	0.8456	9.937	0.381	639.8064	0.3736	9.654	0.371
315.8462	0.8576	9.929	0.377	639.8110	0.3806	9.668	0.378
315.8684	0.8917	9.831	0.367	639.8176	0.3907	9.685	0.379
315.8725	0.8979	9.783	0.357	639.8188	0.3926	9.685	0.380
315.8762	0.9036	9.721	0.340	639.8331	0.4145	9.715	0.384
315.8803	0.9099	9.649	0.334	639.8342	0.4162	9.720	0.388
635.7757	0.1837	9.401	0.309	639.8478	0.4372	9.742	0.391
635.7839	0.1963	9.418	0.313	639.8489	0.4388	9.741	0.392
635.7995	0.2203	9.449	0.326	639.8604	0.4565	9.762	0.389
635.8044	0.2278	9.458	0.328	639.8636	0.4614	9.780	0.394
635.8152	0.2439	9.480	0.334	639.8670	0.4667	9.782	0.397
635.8164	0.2457	9.482	0.336	639.9229	0.5523	9.814	0.395
635.8314	0.2697	9.519	0.342	639.9259	0.5570	9.816	0.392
635.8344	0.2743	9.524	0.346	639.9289	0.5617	9.817	0.391
635.8500	0.2973	9.554	0.357	639.9440	0.5849	9.822	0.391
635.8512	0.2992	9.553	0.351	639.9485	0.5917	9.830	0.393
635.8527	0.3014	9.554	0.355	639.9518	0.5969	9.831	0.397
635.8641	0.3189	9.582	0.359	639.9556	0.6029	9.835	0.396

difficulties. HD 19504 (BD +10°418) is an F star about 21′ north of X Ari, and was the primary comparison star. HD 19431 (BD +9°397) is an A star about 33′ south of X Ari, and was utilized as a check star. The VR_C measurements are given in Table 1, with the Heliocentric Julian Date (HJD) at mid-observation.

TABLE 2

JHK PHOTOMETRY

HJD (−2446000)	Phase	K	J-K	J-H
22.6906	0.3803	7.90	0.38	0.29
22.7010	0.3964	7.89	0.39	0.32
22.7168	0.4206	7.92	0.38	0.32
22.7267	0.4358	7.91	...	...
22.7468	0.4667	7.89	0.38	0.32
22.7552	0.4795	7.92	0.40	0.33
22.7743	0.5089	7.92	0.42	0.34
22.7831	0.5225	7.93	0.41	0.34
22.8192	0.5778	7.96	0.42	0.36
22.8281	0.5915	7.96	0.43	0.35
22.8471	0.6207	7.99	0.42	0.35
22.8559	0.6342	7.99	0.42	0.34
22.8752	0.6640	8.01	0.41	0.34
22.8842	0.6777	8.03	0.41	0.335
22.8934	0.6919	8.03	0.40	0.33
22.9024	0.7056	8.04	0.39	0.33
22.9160	0.7266	8.04	0.39	0.32
22.9244	0.7395	8.045	0.39	0.315
22.9400	0.7634	8.065	0.39	0.32
22.9489	0.7770	8.075	0.39	0.315
23.6347	0.8303	8.12	0.43	0.34
23.6744	0.8912	8.15	0.39	0.30
23.7015	0.9328	8.03	0.285	0.22
23.7074	0.9419	8.02	0.27	0.21
23.7096	0.9452	8.00	0.27	0.20
23.7119	0.9489	8.00	0.26	0.195
23.7168	0.9563	7.98	0.245	0.18
23.7194	0.9603	7.97	0.25	0.19
23.7217	0.9638	7.96	0.23	0.18
23.7240	0.9675	7.93	0.22	0.16
23.7272	0.9723	7.93	0.24	0.18
23.7325	0.9805	7.93	0.21	0.16
23.7353	0.9848	7.91	0.22	0.15
23.7388	0.9902	7.91	0.20	0.15
23.7416	0.9945	7.92	0.20	0.15
23.7452	0.0000	7.88	0.24	0.16
23.7508	0.0086	7.92	0.25	0.21
23.7577	0.0192	7.895	0.24	0.17
23.7600	0.0227	7.895	0.245	0.175
23.7626	0.0266	7.915	0.24	0.19
23.7722	0.0414	7.90	0.26	0.20
23.7867	0.0637	7.90	0.27	0.205
23.7890	0.0673	7.90	0.275	0.21
23.8031	0.0889	7.905	0.29	0.23
23.8188	0.1129	7.90	0.30	0.24
23.8213	0.1168	7.89	0.305	0.25
330.8500	0.6295	7.979	0.415	0.348
330.8696	0.6596	8.016	0.401	0.336
330.8977	0.7027	8.027	0.401	0.323
330.9068	0.7167	8.038	0.396	0.325
331.8629	0.1838	7.865	0.327	0.283
331.8737	0.2001	7.858	0.327	0.285
331.9062	0.2515	7.879	0.356	0.301
331.9430	0.3080	7.870	0.350	0.311
331.9896	0.3796	7.926	0.403	0.312
332.0058	0.4045	7.886	0.407	0.322
332.8094	0.6386	7.994	0.402	0.331
332.8152	0.6475	8.005	0.411	0.339
332.8425	0.6894	8.015	0.397	0.318
332.9097	0.7926	8.101	0.399	0.330
332.9555	0.8630	8.158	0.372	0.308
333.0194	0.9304	8.005	0.262	0.166

During 1984 November 17/18 and 18/19 and 1985 September 21/22, 22/23, and 23/24 we used the KPNO 1.3 m telescope to obtain *JHK* photometry of X Ari and HD 19504. Except for 1985 September 21/22, the nights were photometric, and extinction was measured nightly. Fifteen or more standards from Elias *et al.* (1982) were observed during each night, so the results given in Table 2 are on the "CIT" system. For the one nonphotometric night, only four observations were utilized, when bracketed observations of HD 19504 indicated clear skies. Standard magnitudes were derived using those derived for HD 19504.

To properly phase the infrared observations to the earlier VR_C photometry and radial velocity measures, as well as the unpublished *uvby* photometry of Siegel (1981), we obtained *ubvy* photometry during the 1985 September observing run for X Ari and HD 19504. The weather was photometric, and 12 standards with $V > 6.0$ mag from Crawford and Barnes (1970), Philip and Philip (1973), and Grønbech, Olsen, and Strömgren (1976) were observed. The observations spanned maximum light on the night 1985, September 16/17, and since the *y* filter closely matches the Johnson *V* filter, we were able to phase the data to the previous VR_C results as well as the *JHK* data obtained shortly thereafter. Results are given in Table 3. In Table 4 we give the data of M. Siegel, who used the KPNO No. 4 0.4 m telescope.

HD 19504 was, as we have noted, the primary comparison star. Our 10 *uvby* observations yielded $V = 7.286 \pm 0.001$ mag, $b - y = 0.281 \pm 0.001$ mag, $m_1 = 0.153 \pm 0.002$ mag, and $c_1 = 0.517 \pm 0.002$ mag. The 22 *JHK* observations yielded $K = 6.212 \pm 0.002$ mag, $J-H = 0.197 \pm 0.002$ mag, and $J-K = 0.233 \pm 0.002$ mag. Errors are those of the mean. The *K* magnitudes obtained in 1985 differed by 0.006 mag from the 1984 results, while the $J-H$ and $J-K$ color indices agreed to within 0.001 mag for the two runs. The 44 total VR_C measures of HD 19504 yielded $V = 7.290 \pm 0.01$ mag and $V-R_C = 0.257 \pm 0.001$ mag, while the 31 measures of HD 19431 yielded $V = 7.907 \pm 0.001$ mag and $V-R_C = 0.160 \pm 0.002$ mag. The averages for each star agreed to within 0.002 mag in *V* and $V-R_C$ for the two separate runs, and the error per observation was less than 0.003 mag in $V-R_C$.

The observations were originally phased according to the

TABLE 3

uvby PHOTOMETRY

HJD (−2,446,320)	Phase	*V*	$b-y$	m_1	c_1
5.8623	0.9697	9.051	0.262	0.051	1.117
5.8721	0.9848	8.967	0.243	0.054	1.191
5.8764	0.9914	8.953	0.237	0.058	1.225
5.8870	0.0077	8.953	0.239	0.047	1.268
5.8913	0.0143	8.962	0.243	0.042	1.264
5.9049	0.0352	9.016	0.251	0.040	1.266
5.9094	0.0421	9.033	0.256	0.034	1.267
5.9183	0.0557	9.070	0.264	0.034	1.255
5.9248	0.0657	9.104	0.269	0.035	1.228
5.9358	0.0826	9.141	0.283	0.024	1.214
5.9402	0.0894	9.157	0.291	0.018	1.203
5.9513	0.1064	9.201	0.302	0.014	1.176
5.9553	0.1126	9.220	0.304	0.016	1.156
5.9731	0.1245	9.270	0.326	0.007	1.108
5.9774	0.1465	9.289	0.323	0.017	1.080
5.9952	0.1738	9.334	0.344	0.011	1.048
5.9994	0.1803	9.352	0.346	0.011	1.032

TABLE 4

SIEGEL *uvby* PHOTOMETRY

HJD (-2444000)	Phase	y	b-y	m_1	c_1
566.7480	0.443	9.74	0.437	-0.021	0.725
566.7583	0.459	9.75	0.435	0.015	0.674
566.7644	0.468	9.77	0.431	0.008	0.691
566.7779	0.489	9.79	0.448	-0.024	0.703
566.7873	0.504	9.79	0.449	-0.018	0.679
566.7980	0.520	9.80	0.442	-0.003	0.694
566.8172	0.550	9.82	0.443	0.005	0.656
566.8218	0.557	9.82	0.454	-0.008	0.659
568.7568	0.528	9.81	0.453	-0.016	0.666
568.7689	0.547	9.82	0.452	-0.014	0.640
568.7746	0.556	9.82	0.440	0.008	0.645
568.7849	0.571	9.82	0.453	-0.023	0.650
568.8048	0.602	9.84	0.448	-0.019	0.674
568.8380	0.653	9.84	0.431	0.015	0.653
568.8471	0.667	9.82	0.447	-0.012	0.658
568.8787	0.715	9.84	0.444	-0.024	0.658
568.9050	0.756	9.84	0.413	0.027	0.681
568.9301	0.794	9.88	0.455	-0.043	0.688
568.9389	0.808	9.88	0.456	-0.053	0.702
568.9477	0.821	9.94	0.417	0.035	0.666
568.9555	0.833	9.94	0.443	-0.008	0.622
568.9655	0.849	9.95	0.456	-0.090	0.724
568.9699	0.856	9.94	0.429	0.007	0.621
569.7269	0.018	9.02	0.245	0.019	1.260
569.7300	0.023	9.06	0.256	0.018	1.248
569.7368	0.033	9.07	0.254	0.009	1.270
569.7491	0.052	9.15	0.273	-0.014	1.251
569.7531	0.058	9.14	0.255	0.022	1.257
569.7625	0.073	9.15	0.268	0.020	1.232
569.7713	0.086	9.20	0.286	0.006	1.191
569.7900	0.115	9.28	0.317	-0.036	1.176
569.8046	0.137	9.29	0.316	0.010	1.085
570.7759	0.629	9.85	0.445	0.001	0.646
570.7909	0.652	9.86	0.455	-0.040	0.687
570.8045	0.673	9.86	0.444	0.012	0.631
570.8256	0.705	9.85	0.422	0.048	0.618
570.8379	0.724	9.85	0.447	-0.022	0.654
570.8558	0.752	9.83	0.440	-0.066	0.753
570.8615	0.761	9.84	0.420	-0.011	0.703
570.8717	0.776	9.86	0.418	0.024	0.674
570.8913	0.806	9.91	0.422	-0.002	0.711
570.9032	0.825	9.95	0.407	0.017	0.704
570.9134	0.840	9.96	0.423	0.015	0.689
570.9194	0.850	9.99	0.437	-0.039	0.717
570.9284	0.863	9.98	0.450	-0.031	0.655
570.9361	0.875	9.97	0.450	-0.033	0.643
370.9426	0.885	9.96	0.463	-0.065	0.648
571.8046	0.209	9.45	0.362	0.002	0.940
571.8107	0.218	9.45	0.370	-0.017	0.950
571.8148	0.225	9.46	0.366	0.001	0.936
571.8185	0.230	9.48	0.380	-0.025	0.919
571.8385	0.261	9.51	0.385	-0.008	0.887
571.8489	0.277	9.53	0.387	0.000	0.851
571.8549	0.286	9.54	0.394	0.001	0.839
571.8685	0.307	9.58	0.404	-0.007	0.823
571.8819	0.328	9.61	0.428	-0.058	0.824
571.8861	0.334	9.60	0.424	-0.008	0.761
571.8987	0.353	9.65	0.411	-0.011	0.809
571.9082	0.368	9.67	0.399	0.041	0.717
571.9156	0.379	9.69	0.420	0.016	0.715
571.9232	0.391	9.70	0.416	-0.002	0.771
571.9364	0.411	9.72	0.437	-0.032	0.712
572.8767	0.855	9.97	0.427	-0.006	0.690
572.8872	0.872	9.96	0.445	-0.032	0.659
572.9004	0.892	9.92	0.434	-0.019	0.670
572.9047	0.898	9.90	0.413	0.037	0.606
572.9138	0.912	9.82	0.420	-0.005	0.621
572.9181	0.919	9.75	0.410	-0.008	0.627
572.9224	0.926	9.66	0.381	0.012	0.607
572.9266	0.932	9.55	0.392	-0.013	0.592
572.9306	0.938	9.44	0.345	0.049	0.643
572.9349	0.945	9.38	0.331	-0.006	0.764
572.9400	0.953	9.32	0.333	-0.012	0.826

TABLE 4—*Continued*

HJD (-2444000)	Phase	y	b-y	m_1	c_1
572.9452	0.961	9.25	0.306	0.025	0.870
572.9492	0.967	9.19	0.288	0.027	0.945
572.9528	0.972	9.15	0.269	0.025	1.008
572.9569	0.979	9.09	0.254	0.051	1.031
572.9625	0.987	9.04	0.257	-0.004	1.109
572.9665	0.993	9.01	0.238	0.037	1.103
572.9710	0.000	8.97	0.276	-0.012	1.147
575.7972	0.341	9.62	0.424	-0.033	0.810
575.8060	0.354	9.65	0.413	-0.005	0.777
575.8104	0.361	9.66	0.421	-0.016	0.772
575.8352	0.399	9.72	0.415	0.007	0.742
575.8434	0.412	9.72	0.434	-0.011	0.724
575.8583	0.435	9.75	0.430	0.001	0.715

ephemeris of Zessewitch, Firmaniuk, and Kreiner (1982),

$$\text{HJD(max light)} = 2{,}437{,}583.570 + 0.6511426E \ . \quad (1)$$

However, maximum light for the 1982 observations occurred at a predicted phase of 0.085, indicating a problem with this ephemeris. Siegel (1980) mentions X Ari as an example of a variable with a secularly increasing period, so that a quadratic term should be introduced into the ephemeris, such that

$$\text{HJD(max light)} = \text{HJD(zero point)} + P_0(1 + \tfrac{1}{2}\beta E)E \ , \quad (2)$$

where P_0 is the value of the period in days at $E = 0$. Further analysis of the times of maximum light observed not only by this investigation but also by Siegel (1981) and Manduca *et al.* (1981) show that the ephemeris of X Ari is best described by

$$\text{HJD(max light)} = 2{,}446{,}325.8820 + (0.6511571)(1 + \tfrac{1}{2}\beta E)E \ , \quad (3)$$

with $\beta = 1.66 \times 10^{-9}$ days days^{-1}. Tables 1–4 list the photometric observations along with this phasing, while Figures 1–4 plot V, J and K, $b - y$, and $V - R_C$, respectively, versus phase.

b) Radial Velocities

The radial velocities were obtained by D. W. L. during 1983 October 26–November 2 (simultaneous with the second VR_C photometry run) with the 1.55 m reflector at the Oak Ridge Observatory at Harvard, Massachusetts. The technique involved the use of an echelle spectrograph and photon-counting Reticon to record 50 Å of a spectrum centered at 5190 Å, at a dispersion of 2.2 Å mm^{-1} and with a resolution of 10 km s^{-1}. Each exposure was cross-correlated against a high signal-to-noise spectrum of a comparison star (see Latham 1985 and Wyatt 1985 for more details). Table 5 lists the HJD and phase at midexposure, final heliocentric velocities, and the internal error estimates, while Figure 5 depicts the radial velocity versus phase. The actual errors are perhaps a factor of 2 greater than the internal estimates (CL), but the former are still less than 1 km s^{-1} most of the time.

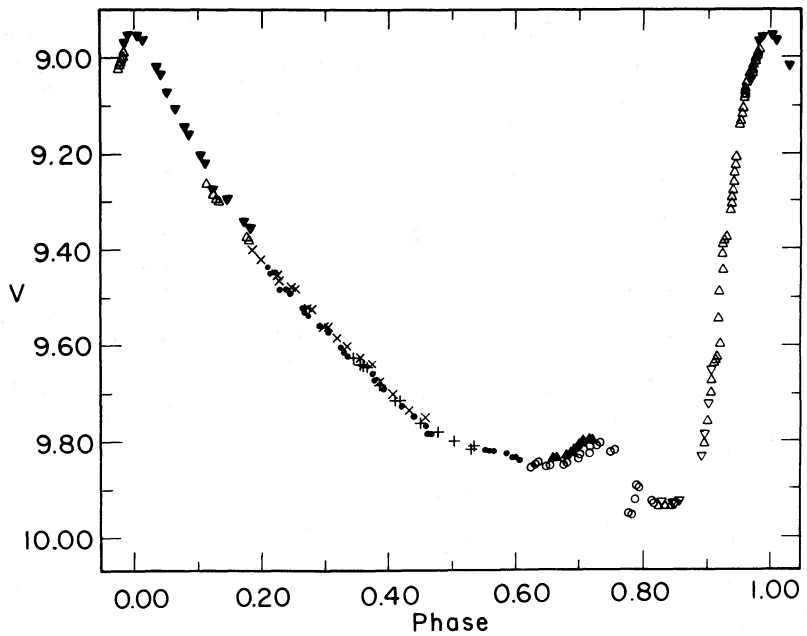

FIG. 1.—V magnitudes of X Ari from Tables 1 and 3 plotted against phase. The symbols refer to data obtained on the following nights: 1982 December 5/6 (*filled triangles*); 1982 December 6/7 (*open triangles*); 1982 December 11/12 (*inverted open triangles*); 1983 October 27/28 (*crosses*); 1983 October 28/29 (*open circles*); 1983 October 29/30 (*plus signs*); 1983 October 31/November 1 (*filled circles*); 1985 September 16/17 (*inverted filled triangles*).

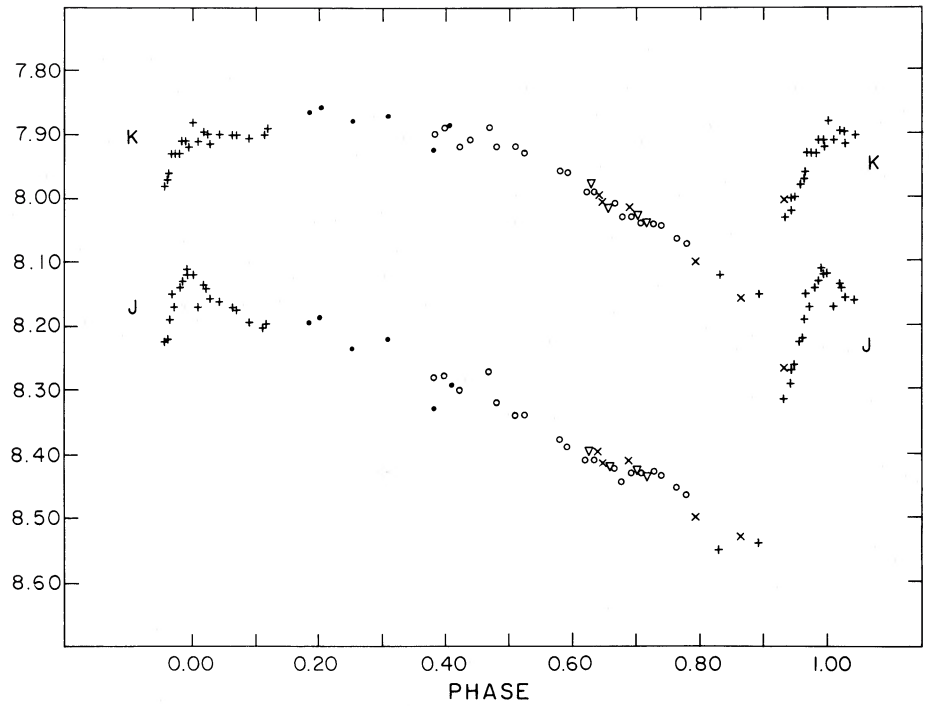

FIG. 2.—*J* (*bottom*) and *K* (*top*) magnitudes of X Ari from Table 2. Symbols are for data from the following nights: 1984 November 17/18 (*open circles*); 1984 November 18/19 (*plus signs*); 1985 September 21/22 (*inverted open triangles*); 1985 September 22/23 (*filled circles*); 1985 September 23/24 (*crosses*).

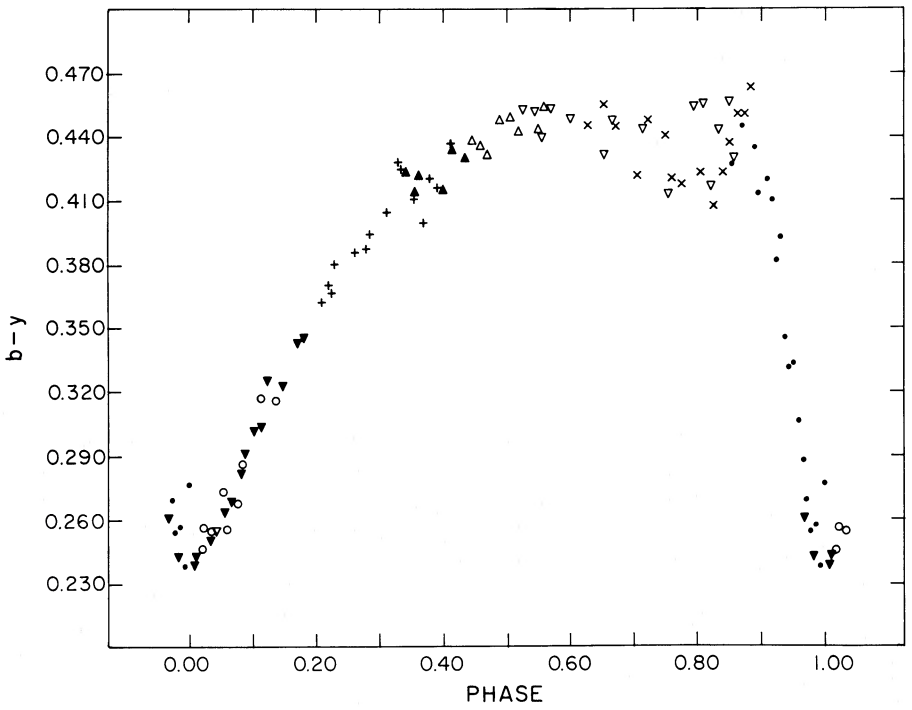

FIG. 3.—($b - y$) colors of X Ari from Tables 3 and 4. Symbols are as follows: 1980 November 22/23 (*open triangles*); 1980 November 24/25 (*inverted open triangles*); 1980 November 25/26 (*open circles*); 1980 November 26/27 (*crosses*); 1980 November 27/28 (*plus signs*); 1980 November 28/29 (*filled circles*); 1980 December 1/2 (*filled triangles*); 1985 September 16/17 (*inverted filled triangles*).

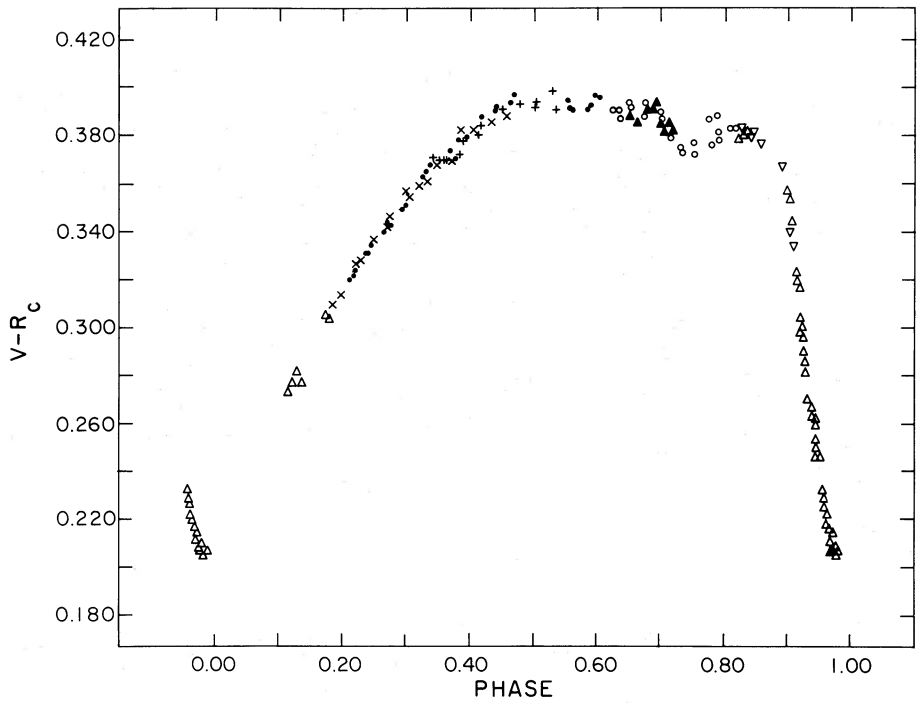

FIG. 4.—$V-R_C$ colors of X Ari from Table 1. Symbols are the same as for Fig. 1.

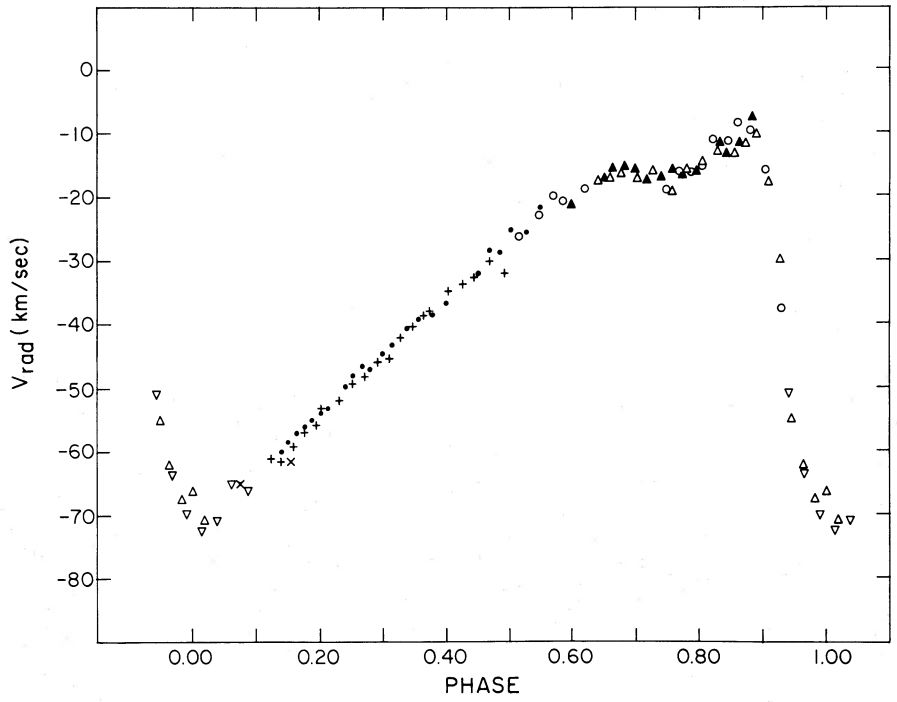

FIG. 5.—Radial velocities of X Ari from Table 5. Symbols are the same as for Fig. 1, except for 1983 October 26/27 (*filled triangles*); 1983 October 30/31 (*open triangles*); 1983 November 1/2 (*inverted open triangles*).

TABLE 5

RADIAL VELOCITIES

HJD (−2445600)	Phase	v_{rad} (km/sec)	σ (km/sec)	HJD −2445600)	Phase	v_{rad} (km/sec)	σ (km/sec)
34.7437	0.5988	−21.27	0.79	38.6800	0.6437	−17.63	0.45
34.7725	0.6425	−17.33	0.67	38.6916	0.6615	−16.70	0.56
34.7857	0.6628	−15.74	0.70	38.7036	0.6799	−16.12	0.51
34.7977	0.6812	−15.50	0.64	38.7189	0.7034	−16.98	0.63
34.8098	0.6998	−16.49	0.61	38.7341	0.7268	−16.10	0.58
34.8217	0.7181	−17.62	0.72	38.7519	0.7541	−19.27	0.64
34.8345	0.7378	−17.18	0.61	38.7696	0.7813	−16.33	0.60
34.8465	0.7562	−16.06	0.74	38.7856	0.8059	−14.90	0.61
34.8584	0.7745	−16.79	0.59	38.8007	0.8290	−13.13	0.52
34.8710	0.7938	−16.23	0.68	38.8158	0.8522	−13.31	0.66
34.8921	0.8262	−11.71	0.75	38.8281	0.8711	−11.86	0.63
34.9042	0.8448	−13.31	0.96	38.8397	0.8889	−10.57	0.79
34.9165	0.8637	−11.86	0.87	38.8514	0.9069	−17.97	0.65
34.9283	0.8818	− 7.88	1.02	38.8650	0.9278	−30.12	1.53
35.7031	0.0722	−65.20	0.72	38.8766	0.9459	−54.98	1.10
35.7571	0.1546	−61.67	0.96	38.8883	0.9636	−62.30	0.99
36.6478	0.5227	−26.37	0.56	38.8999	0.9814	−67.59	1.29
36.6632	0.5464	−22.99	0.49	38.9112	0.9994	−66.25	1.49
36.6788	0.5703	−19.92	0.75	38.9232	0.0172	−71.02	0.88
36.6892	0.5863	−20.61	0.87	39.6533	0.1387	−60.09	0.60
36.7122	0.6216	−18.83	0.61	39.6615	0.1510	−58.65	0.56
36.7956	0.7497	−19.25	0.61	39.6697	0.1636	−57.42	0.47
36.8080	0.7687	−16.20	0.64	39.6782	0.1767	−56.20	0.48
36.8196	0.7866	−16.56	0.73	39.6864	0.1893	−55.18	0.52
36.8317	0.8051	−15.75	0.72	39.6946	0.2019	−53.96	0.55
36.8437	0.8236	−11.33	0.65	39.7028	0.2145	−53.42	0.63
36.8568	0.8437	−11.62	0.83	39.7116	0.2280	−52.34	0.46
36.8685	0.8616	− 8.63	0.54	39.7199	0.2407	−49.85	0.49
36.8808	0.8805	−10.04	0.73	39.7281	0.2533	−48.05	0.53
36.8964	0.9045	−16.19	1.16	39.7366	0.2664	−46.88	0.37
36.9117	0.9280	−37.82	1.28	39.7448	0.2790	−47.27	0.43
37.6890	0.1220	−61.18	0.66	39.7575	0.2985	−44.89	0.43
37.7008	0.1399	−61.83	0.49	39.7688	0.3158	−43.51	0.44
37.7125	0.1578	−59.23	0.59	39.7833	0.3381	−40.82	0.48
37.7243	0.1760	−57.10	0.63	39.7950	0.3561	−39.39	0.41
37.7362	0.1942	−55.71	0.52	39.8096	0.3785	−38.49	0.44
37.7480	0.2124	−53.63	0.60	39.8237	0.4001	−34.48	0.55
37.7600	0.2308	−52.02	0.55	39.8417	0.4278	−33.79	0.39
37.7744	0.2529	−49.58	0.52	39.8560	0.4497	−32.26	0.52
37.7862	0.2710	−48.32	0.50	39.8777	0.4677	−28.55	0.61
37.7994	0.2913	−46.09	0.51	39.8794	0.4857	−28.74	0.64
37.8112	0.3094	−45.37	0.60	39.8910	0.5035	−25.51	0.82
37.8231	0.3277	−42.12	0.53	39.9063	0.5270	−25.77	0.56
37.8348	0.3457	−40.67	0.54	39.9215	0.5503	−21.88	0.59
37.8466	0.3638	−38.98	0.51	40.8274	0.9416	−51.02	0.91
37.8585	0.3821	−37.47	0.64	40.8432	0.9658	−63.59	0.95
37.8722	0.4031	−34.89	0.55	40.8587	0.9896	−69.76	0.95
37.8875	0.4266	−33.84	0.47	40.8740	0.0131	−72.22	0.73
37.8993	0.4447	−32.61	0.64	40.8900	0.0377	−70.71	0.67
37.9195	0.4681	−30.20	0.57	40.9057	0.0618	−65.09	0.94
37.9298	0.4916	−32.10	0.76	40.9212	0.0858	−65.87	1.07

TABLE 6

OBSERVED ECHELLE ORDERS IN HIGH-DISPERSION SPECTRA

Order	Central Wavelength (Å)	Order	Central Wavelength (Å)
121.....	4602	127.....	4385
122.....	4563	128.....	4351
123.....	4529	129.....	4315
124.....	4490	130.....	4281
125.....	4455	131.....	4250
126.....	4419	132.....	4220

TABLE 7

HIGH-DISPERSION SPECTRA: X ARI

Spectrum Number	HJD (midexposure)	Phase (midexposure)	Exposure Time	
			Seconds	Phase
2005.....	2,445,918.9226	0.021	1800	0.032
2007.....	2,445,918.9632	0.083	2400	0.043
2013.....	2,445,919.9138	0.543	3600	0.064
2018.....	2,445,920.9569	0.145	3600	0.064

In order to check for the existence of a velocity gradient in the stellar atmosphere that would distort the radial velocity values, four high-dispersion (= 2.2 Å mm^{-1} at Hγ) spectra of X Ari were obtained at Kitt Peak National Observatory over the interval of 1984 August 5–7, using the 4 m reflector. A 12 mm × 12 mm TI CCD (No. 3) was used in conjunction with the 31 lines mm^{-1} echelle grating, the 226-2 cross-dispersion grating, and the long red camera to observe 12 orders (Table 6), with the orders aligned along the CCD columns. Table 7 lists the exposure times and phases of the observations. Each exposure was bracketed by 20 minute exposures of the Th-Ar comparison lamp in order to monitor the effects of flexure of the instrument on the spectra. The CCD was preflashed for 4 s by a quartz lamp for each comparison exposure in order to minimize charge transfer problems, and we employed 2 pixel summation of the rows to reduce the readout noise.

III. ANALYSIS AND RESULTS

a) Overview of the Algebraic and Surface Brightness Methods

The procedure followed in this analysis is the same as that employed by CL for their analysis of VY Ser. Basically, it consists of the application of two variations of the Baade-Wesselink method, the algebraic method and the surface brightness method.

The algebraic method determines the absolute brightness by first solving for the radius and then using computed values of the effective temperature from model atmospheres to calculate the luminosity as a function of phase. The equation

$$\langle R(\phi_1)\rangle = \langle \Delta R_{\rm spect}(\phi_1, \phi_2)/[r(\phi_1, \phi_2) - 1]\rangle_\phi , \quad (4)$$

where the change in the "spectroscopic radius," $\Delta R_{\rm spect}$, is defined as

$$\Delta R_{\rm spect}(\phi_1, \phi_2) = R(\phi_2) - R(\phi_1) = -\int_{t_1}^{t_2} v_p\, dt$$

$$= -\int_{\phi_1}^{\phi_2} p(v_{\rm rad} - \gamma) P d\phi \quad (5)$$

and the ratio r of the "photometric radii" is

$$r(\phi_1, \phi_2) = \frac{R_{\rm phot}(\phi_2)}{R_{\rm phot}(\phi_1)}$$

$$= \left[\frac{T_{\rm eff}(\phi_1)}{T_{\rm eff}(\phi_2)}\right]^2 {\rm dex}\,\{-0.2[m_{\rm bol}(\phi_2) - m_{\rm bol}(\phi_1)]\} , \quad (6)$$

is used to find the value of the radius R at some reference phase ϕ_1 by averaging over all subsequent pairs to some later phase ϕ_f. The value of p, the correction factor to convert radial velocities $v_{\rm rad}$ to pulsational velocities v_p, is again assumed to be 1.30, while the value of the systematic velocity γ for X Ari is calculated by integrating the velocity curve over the full cycle. The period P chosen is the value P_0 in equation (3); the results are not affected significantly by the varying period as long as the phasing is correct, because of the near-simultaneity of the photometric and spectroscopic observations. Values of the radius at the other phases are calculated simply from

$$R(\phi_2) = R(\phi_1) + \Delta R_{\rm spect}(\phi_1, \phi_2) . \quad (7)$$

The observed data were smoothed into bins of 0.01 in phase, and the values of the derivative and the integral of $v_{\rm rad}$ with respect to ϕ were obtained by the use of local cubic splines (see Thompson 1984 for more details about this type of analysis). The value of the systemic velocity γ was calculated from the integrated splines and equation (5), and the value $\gamma = -36.9 \pm 0.2$ km s^{-1} is adopted for X Ari.

In order to convert the observed magnitudes and colors to effective temperatures and bolometric magnitudes, it is necessary to know the value of the interstellar reddening. Following the lead of Manduca *et al.* (1981), we will adopt the value of $E(B-V) = 0.153$ mag, which is an average of the values 0.149 mag (Lub 1977) and 0.157 mag (Burstein and Heiles 1978). The values of $T_{\rm eff}$ and the bolometric correction BC in a given filter are then obtained by comparing the unreddened colors with synthetic colors taken from the unpublished values of R. L. Kurucz, who computed them from atomic line-blanketed models with $\alpha = 1$ ($\alpha \equiv$ the ratio of convective mixing length to pressure scale height). As in CL, the zero points of the synthetic colors were checked by comparing the computed and observed colors of Procyon, and again no zero-point shift was required in the synthetic colors. However, the synthetic BC values had to be fitted by +0.240 mag, as discussed by CL. Because the synthetic values are sensitive to metallicity, the correct values for X Ari were obtained by interpolating between Kurucz's [M/H] = −2 and −2.5 models, since X Ari has a value of [Fe/H] = −2.17 (Butler 1975). Tables 8 and 9 list the values of the adopted synthetic colors and synthetic BCs, respectively. Since the synthetic JK values are on the Johnson system, the observed "CIT" colors were transformed to this system using relations derived from Elias *et al.* (1983), assuming that the AAO system is the same as the Johnson system (Griersmith, Hyland, and Jones 1982; Jones and Hyland 1983):

$$(V-K)_J = (V-K)_{\rm CIT} - 0.011 , \quad (8)$$

$$(J-K)_J = [(J-K)_{\rm CIT} - 0.006]/0.897 . \quad (9)$$

The synthetic values are also gravity-sensitive, so some means of estimating the effective gravity $g_{\rm eff}$, defined by

$$\log g_{\rm eff} = \log\left(\frac{GM}{R^2} + \frac{dv_p}{dt}\right) , \quad (10)$$

is required. Thus, the radius must be determined by an iteration process. A starting log $g_{\rm eff}$ (usually 2.5, although the results are not sensitive to this) is chosen, values of $T_{\rm eff}$ and BC are then computed, and the radius as a function of phase is determined using equations (4)–(7). These values are then utilized to estimate log $g_{\rm eff}$ from equation (10), assuming a mass of 0.6 $M_\odot$ and the process is repeated until convergence is reached, which generally involves no more than four iterations. In order to avoid possible distortion of the colors as a result of shock waves and rapidly changing opacity, the phase interval was restricted to $0.15 \le \phi \le 0.60$. Also, a lower limit to the value $|r - 1|$ was set at 10^{-4} in order to avoid computational instabilities.

The other version of the Baade-Wesselink method considered here is the surface brightness method, which was first devised by Wesselink (1969) and was reformulated by Manduca and Bell (1981). The surface brightness of a star in the V filter is defined to be

$$S_V = V_0 + 5\log\theta_{\rm phot}$$

$$= {\rm constant} - ({\rm BC})_V - 10\log T_{\rm eff} , \quad (11)$$

where $\theta_{\rm phot}$ is the angular diameter in milliarcseconds, so that

$$5\log\theta_{\rm phot} = {\rm constant} - [V_0 + ({\rm BC})_V] - 10\log T_{\rm eff} , \quad (12)$$

TABLE 8

SYNTHETIC COLORS [M/H] = −2.2

COLOR	EFFECTIVE TEMPERATURE (K) 5500	6000	6500	7000	7500	8000
			log g = 1.0			
$B-V$	0.527	0.369	0.235	0.101	0.029	...
$b-y$	0.390	0.287	0.197	0.108	0.062	...
$V-R_C$	0.373	0.281	0.197	0.121	0.067	...
$V-K$	1.680	1.299	0.964	0.682	0.455	...
$J-K$	0.455	0.343	0.246	0.171	0.118	...
			log g = 1.5			
$B-V$	0.521	0.378	0.259	0.135	0.041	−0.005
$b-y$	0.388	0.294	0.211	0.127	0.065	0.036
$V-R_C$	0.375	0.289	0.208	0.134	0.074	0.038
$V-K$	1.701	1.329	0.998	0.712	0.479	0.306
$J-K$	0.467	0.354	0.257	0.178	0.110	0.079
			log g = 2.0			
$B-V$	0.520	0.388	0.278	0.175	0.067	0.006
$b-y$	0.389	0.301	0.224	0.150	0.076	0.036
$V-R_C$	0.377	0.297	0.220	0.148	0.085	0.041
$V-K$	1.719	1.357	1.032	0.742	0.505	0.320
$J-K$	0.476	0.365	0.268	0.185	0.124	0.080
			log g = 2.5			
$B-V$	0.523	0.400	0.297	0.205	0.109	0.031
$b-y$	0.391	0.309	0.236	0.169	0.098	0.044
$V-R_C$	0.380	0.304	0.232	0.163	0.100	0.049
$V-K$	1.736	1.385	1.065	0.776	0.531	0.358
$J-K$	0.483	0.374	0.277	0.193	0.129	0.081
			log g = 3.0			
$B-V$	0.528	0.412	0.315	0.231	0.151	0.064
$b-y$	0.394	0.318	0.249	0.185	0.122	0.059
$V-R_C$	0.383	0.310	0.243	0.178	0.115	0.061
$V-K$	1.747	1.409	1.098	0.813	0.561	0.362
$J-K$	0.488	0.383	0.287	0.203	0.133	0.084
			log g = 3.5			
$B-V$	0.538	0.423	0.331	0.253	0.183	0.110
$b-y$	0.400	0.326	0.261	0.200	0.142	0.084
$V-R_C$	0.386	0.317	0.253	0.191	0.131	0.076
$V-K$	1.752	1.430	1.130	0.851	0.598	0.386
$J-K$	0.489	0.391	0.297	0.213	0.141	0.087
			log g = 4.0			
$B-V$	0.549	0.435	0.346	0.273	0.209	0.148
$b-y$	0.407	0.334	0.272	0.214	0.159	0.107
$V-R_C$	0.391	0.321	0.261	0.203	0.146	0.092
$V-K$	1.749	1.444	1.157	0.888	0.638	0.416
$J-K$	0.485	0.396	0.307	0.225	0.152	0.091
			log g = 4.5			
$B-V$	0.562	0.448	0.360	0.290	0.231	0.178
$b-y$	0.415	0.343	0.282	0.227	0.175	0.126
$V-R_C$	0.395	0.327	0.268	0.213	0.160	0.108
$V-K$	1.740	1.450	1.180	0.922	0.679	0.457
$J-K$	0.478	0.398	0.316	0.237	0.164	0.101

or

$$\theta_{phot} = \text{dex}\,[0.2(\text{constant} - m_{bol} - 10 \log T_{eff}]\,. \quad (13)$$

The value of the constant is again taken to be 42.160 as discussed by CL. In order to calculate m_{bol} and T_{eff}, a value of log g_{eff} at a reference phase ϕ_1 is assumed, and equations (5), (7), and (10) are then applied to generate the radii and values of log g_{eff} at all other phases, which are then employed to compute the variation of m_{bol} and T_{eff} with phase. The photometric angular diameter θ_{phot} is found as a function of phase from equation (13), and the spectroscopic angular diameter θ_{spect} is obtained from the radius by multiplying by 2 and dividing by the assumed distance. The values of the distance and log $g_{eff}(\phi_1)$ are adjusted until the variation of θ_{spect} with phase matches that of θ_{phot}. This method has distinct advantages over the algebraic method, in that phasing problems are readily apparent and also there is no chance of numerical instability as in the algebraic method.

It was discovered in the S_V analysis of VY Ser (CL) that the radial velocities had to be shifted in phase by +0.075 (or the photometry had to be shifted by −0.075) in order for the variation of θ_{spect} versus phase to match that of θ_{phot}. The same phase shift was also required for the algebraic method. When these methods were first applied to X Ari, using simultaneous VR_C photometry and spectroscopy, a smaller but still significant phase shift was needed as well (see § III*c* below), indicating a problem with the Baade-Wesselink method itself instead of one associated with the fact that VY Ser is located near the red edge of the instability strip. This problem has two possible causes: (1) the distortion of the radial velocity curve and the value of the systemic velocity due to the presence of a velocity gradient in the stellar atmosphere along with a variation of opacity with phase, and (2) problems with the color-temperature conversions.

b) Analysis of Possible Radial Velocity Distortion

OGS first discussed the radial velocity difficulties in their study of SU Dra. As can be seen in their Figure 3, velocities derived from the hydrogen lines show a greater variation with phase than those from metal lines, an effect also noted by Sanford (1949). Since the hydrogen lines form at a higher atmospheric level than do the metal lines, this indicates that there is a velocity gradient present in RR Lyrae stars, at all phases. Since the radial velocities are obtained from absorption lines which form above the photosphere, the assumption of the Baade-Wesselink method that the radial velocity curve represents the motion of the photosphere may not be valid. Furthermore, since the opacity of the star changes because of the variation of T_{eff} and log g_{eff}, the lines form in different layers in the atmosphere at different times. Since the computation of γ by the integration of the radial velocity curve assumes that the velocity variation is that of a single layer, this opacity change may lead to an incorrect value of γ. OGS compensated for this by noting that, for SU Dra, the opacity is roughly constant from phase 0.40 to phase 0.85, and thus the velocities come from the same layer in this interval. They used these metal-line velocity values to extrapolate a line back in phase from 0.40 to represent the motion of this layer. The resulting velocity curve is less blueshifted in the phase interval 0.90–0.40 than the one derived from the metal lines, and if γ is calculated from this curve, it will be more positive than the one from the metal-line observations. Since maximum radius occurs at a phase when $v_{rad} = \gamma$, a more positive γ causes maximum radius to occur at a later phase, or, conversely, the γ calculated from the metal-line curve causes the maximum radius calculated from spectroscopy to appear to occur at an earlier phase than it actually does. This is exactly the situation encountered in VY Ser and X Ari: the maximum radius obtained from spectroscopy is at an earlier phase compared with that of photometry.

TABLE 9

SYNTHETIC BOLOMETRIC CORRECTIONS[a]: [M/H] = −2.2

log g	BC	Effective Temperature (K) 5500	6000	6500	7000	7500	8000
1.0.....	$(BC)_V$	−0.143	−0.043	0.024	0.053	0.053	...
	$(BC)_K$	1.537	1.256	0.988	0.735	0.508	...
1.5.....	$(BC)_V$	−0.162	−0.067	0.002	0.040	0.044	0.010
	$(BC)_K$	1.539	1.262	1.000	0.752	0.523	0.136
2.0.....	$(BC)_V$	−0.182	−0.093	−0.024	0.022	0.029	0.006
	$(BC)_K$	1.537	1.264	1.008	0.764	0.534	0.326
2.5.....	$(BC)_V$	−0.200	−0.119	−0.054	−0.005	0.012	−0.007
	$(BC)_K$	1.536	1.266	1.011	0.771	0.543	0.331
3.0.....	$(BC)_V$	−0.214	−0.143	−0.084	−0.037	−0.010	−0.026
	$(BC)_K$	1.533	1.266	1.014	0.776	0.551	0.336
3.5.....	$(BC)_V$	−0.222	−0.164	−0.115	−0.072	−0.042	−0.042
	$(BC)_K$	1.530	1.266	1.015	0.779	0.556	0.344
4.0.....	$(BC)_V$	−0.225	−0.178	−0.141	−0.106	−0.078	−0.067
	$(BC)_K$	1.524	1.266	1.016	0.782	0.560	0.349
4.5.....	$(BC)_V$	−0.224	−0.184	−0.160	−0.137	−0.116	−0.103
	$(BC)_K$	1.516	1.266	1.020	0.785	0.563	0.354

[a] $(BC)_K$ values were computed from synthetic $V-K$; $(BC)_V$, by $(BC)_K = (BC)_V + (V-K)$.

In order to test this idea, four high-dispersion spectra of X Ari were obtained, three at phases of rapidly changing opacity and the fourth at a phase within the constant-opacity phase interval, which for X Ari is the region $0.40 \leq \phi \leq 0.60$, in order to measure velocities of lines at different depths of formation. A second-order dispersion solution was fitted to each order of each comparison spectrum by using weighted least squares on the observed comparison lines. The centroids of these lines were found by a parabolic fit to the line, again by weighted least squares, while the corresponding wavelength values were obtained from Chaffee and Peters (1983). The centroid of each unblended absorption line in the stellar spectra was also derived by a parabolic fit, and the corresponding wavelength value was derived from the dispersion solutions of the bracketing comparison spectra. These wavelengths yielded the radial velocities when compared with the unshifted values of Moore, Minnaert, and Houtgast (1966). The velocity difference with respect to the line Fe I λ4383.557, which forms at the highest level in the atmosphere, was calculated for each line, instead of the absolute value of the velocity, in order to minimize zero-point errors. Table 10 lists the velocity differences for these lines, along with the errors. The error in the velocity for each absorption line was computed from the error in the centroid of the line in the stellar spectrum and from the uncertainty in the wavelength as derived from the dispersion solution, and the errors in the velocity difference were obtained by adding the error of each line involved quadratically with that of the reference Fe I line. Figure 6 plots the depth [≡ log (column density)] of the core of each line of Table 10 and also the depth of both the strongest absorption line in the CfA spectra and the "continuum" as a function of phase. These depths were determined from the application of the program WIDTH6 and the Kurucz model atmospheres appropriate to the given phases and the elemental abundances of Butler (1975). The "continuum" values were derived from weak high-excitation lines with a computed equivalent width of less than 0.1 mÅ, which form very deep in the photosphere, and also from the depth of the layer with an optical depth τ_{5000} of unity. It is apparent that there is no significant velocity gradient in this region of the atmosphere, certainly not to the extent suggested by OGS. We thus confirm the results from the models of Christy (1966).

To corroborate these results, the Reticon data of both VY Ser and X Ari were examined using the program GAUSSFIT at the Harvard-Smithsonian Center for Astrophysics. Velocities were measured from absorption lines of various strengths, including the strongest and the weakest lines, in

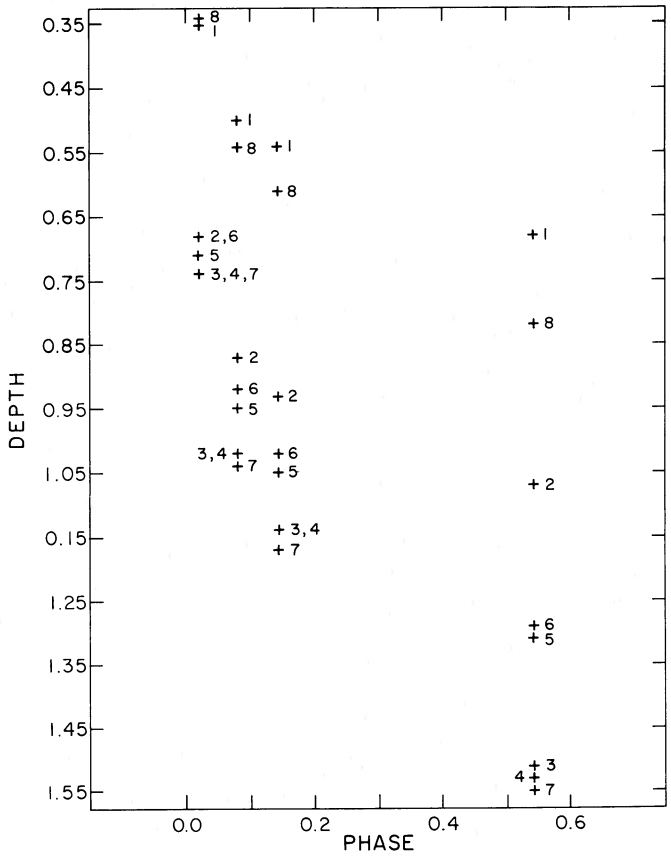

FIG. 6.—Depths [≡ log (column density)] of the cores of spectral absorption lines of X Ari plotted against phase. Numbers refer to the following lines: 1—Fe I λ4383.557; 2—Fe I λ4415.135; 3—Ti II λ4417.723; 4—Fe II λ4555.892; 5—Ti II λ4563.766; 6—Ti II λ4571.982; 7—"continuum"; 8—Mg I λ5183.619 (strongest line of Reticon data).

TABLE 10

VELOCITY DIFFERENCES[a] OF ABSORPTION LINES: KPNO SPECTRA

LINE	SPECTRUM NUMBER 2005 ($\phi = 0.021$)	2007 ($\phi = 0.083$)	2013 ($\phi = 0.543$)	2018 ($\phi = 0.145$)	DESIGNATION IN FIGURE 6
Fe I λ4383.557	0	0	0	0	1
Fe I λ4415.135	0.1 ± 2.3	0.0 ± 2.3	−0.7 ± 2.3	0.1 ± 2.3	2
Ti II λ4571.982	1.5 ± 2.4	1.9 ± 2.4	...	0.7 ± 2.3	6
Ti II λ4563.766	0.6 ± 2.3	2.3 ± 2.3	−1.0 ± 2.3	1.2 ± 2.3	5
Ti II λ4417.723	...	−0.3 ± 2.3	−1.5 ± 2.6	0.9 ± 2.3	3
Fe II λ4555.892	0.7 ± 2.6	0.5 ± 2.6	−0.1 ± 2.6	2.4 ± 2.6	4

[a] Lines are arranged here in order of increasing depth of formation. Velocity difference in km s^{-1} for line $x \equiv v(x) - v$(4383.557 Å line).

exposures from all phases of the pulsation cycle. Table 11 lists these lines along with their ionization stage and excitation potential. Once again, the velocities derived from each line agreed with those of the other lines in each spectrum within the error of 2 km s^{-1}, indicating that no velocity gradient exists, so therefore it can be concluded that the radial velocity curve does represent the photospheric motion and that the value of γ computed from this curve is indeed accurate. This suggests that the cause of the phasing problem lies elsewhere.

c) Examination of the Color-Temperature Transformation

Infrared *JHK* photometry of X Ari was subsequently obtained, and these values were used along with the Strömgren *uvbyβ* data provided by Siegel (1981), *UBV* photometry from Preston and Paczyński (1964) and Sturch (1966), and the previous VR_C photometry in order to test the validity of the calculated effective temperatures and bolometric corrections. Values of $T_{\rm eff}$ and BC for both versions of the Baade-Wesselink method were computed from the $B-V$, $b-y$, $V-R_C$, $V-K$, and $J-K$ indices, and $m_{\rm bol}$ was calculated from both the apparent V magnitudes and the apparent K magnitudes. Results of the algebraic method for the various magnitude-color combinations are found in Table 12; Figure 7 presents the surface brightness results in the phase region $0.15 \leq \phi \leq 0.70$ obtained using the five color indices in conjunction with the V magnitude, and Figure 8 shows the results found using the color indices and the K magnitude. As can be seen, the phasing problem vanishes when the $V-K$ index is used, whereas the problem is greatest for the $B-V$ and $b-y$ values, with each yielding a phase difference as large as that for VY Ser when they are combined with the V filter. There is also a problem with the results obtained from the $J-K$ index and the V magnitude, since these values are anomalously decreasing while the others are increasing. Furthermore, there is a dramatic improvement in both the $b-y$ and the $V-R_C$ results when the K filter is used to determine $m_{\rm bol}$ instead of the V filter. The reason for this becomes apparent when the effective temperatures are considered (Table 13): the various indices yield significantly different temperatures at different phases. It can be seen from equation (13) that in a comparison of two different temperatures at the same phase, the lower temperature will translate into a larger value of $\theta_{\rm phot}$. Also, since the value of BC is estimated from $T_{\rm eff}$ in conjunction with log $g_{\rm eff}$, it can be noted from Table 9 that the value of $(BC)_V$ corresponding to the lower $T_{\rm eff}$ is more negative than the one from the higher $T_{\rm eff}$, while the $(BC)_K$ value is more positive at the lower $T_{\rm eff}$, owing to the shift of the peak of the intensity function toward the longer wavelengths for the cooler temperatures. The result of this is that the $(BC)_V$ value causes the computed $\theta_{\rm phot}$ from the lower $T_{\rm eff}$ to be even larger, while the $(BC)_K$ value tends to cancel out the effect of the lower temperature. It should be noted that the values of $(BC)_K$ in Table 9 were obtained from the synthetic $V-K$ and $(BC)_V$ values, so the results from the V, $V-K$ and the K, $V-K$ combinations are artificially identical. However, this index yields the most symmetric results and is apparently the only one that actually works, so we will adopt the results obtained from this index as our standard. A distance modulus of 8.23 mag was obtained from the surface brightness method in the phase interval $0.15 \leq \phi \leq 0.60$ (Fig. 8), which, when combined with the mean

TABLE 11

ABSORPTION LINES: RETICON ORDER

LINE	EXCITATION POTENTIAL (eV)
Fe II λ5169.050	2.88
Mg I λ5172.698	2.71
Mg I λ5183.619	2.71
Ti II λ5185.908	1.89
Fe I λ5191.465	3.04
Fe I λ5192.353	3.00
Fe I λ5194.949	1.56
Fe II λ5197.576	3.23

TABLE 12

RESULTS OF ALGEBRAIC METHOD: X ARI

COLOR	$\langle M_V \rangle$(mag) $0.15 \leq \phi \leq 0.40$	$0.15 \leq \phi \leq 0.60$
V Magnitude		
$B-V$	1.26	2.53
$b-y$	1.76	2.25
$V-R_C$	0.91	1.42
$V-K$	0.89	0.88
$J-K$	[a]	[a]
K Magnitude		
$B-V$	1.03	1.40
$b-y$	1.13	1.31
$V-R_C$	0.93	1.01
$V-K$	0.89	0.88
$J-K$	[a]	[a]

[a] No convergence.

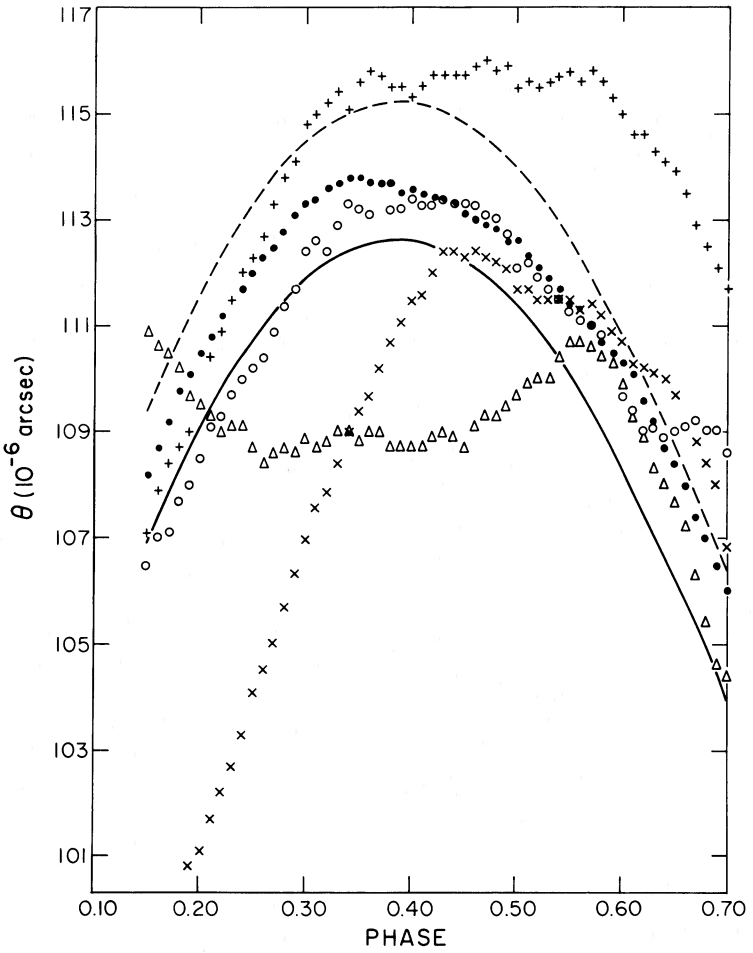

FIG. 7.—Angular diameters (units are 10^{-6} arcsec) obtained via the surface brightness method and the data of Tables 1–5. Lines represent spectroscopic results for $m - M = 8.20$ mag (*dashed lines*) and 8.25 mag (*solid line*). Symbols are angular radii derived from V magnitudes and the following color indices: $V-K$ (*filled circles*); $V-R_C$ (*open circles*); $b-y$ (*plus signs*); $J-K$ (*open triangles*); and $B-V$ (*crosses*).

unreddened apparent magnitude $\langle V_0 \rangle = 9.11$ mag, yields $\langle M_V \rangle = +0.88$ mag, in perfect agreement with the results obtained from the algebraic method in the same phase interval (Table 12).

The phase interval can be divided into three subintervals, based on the behavior of the effective temperature: (1) the region $0.15 \leq \phi \leq 0.40$, where $T_{\rm eff}$ is decreasing with increasing phase, (2) the interval $0.40 \leq \phi \leq 0.60$, which is the region of essentially constant temperature, and (3) the phases $\phi > 0.60$, in which the $T_{\rm eff}$ values are increasing with increasing phase. As can be seen in Table 13, the computed effective temperatures from the $B-V$ and $V-R_C$ indices agree very well with the standard values in region 2, while the values from the $J-K$ index are in agreement with the others for phases $0.50 \leq \phi \leq 0.60$. The values obtained from the $b-y$ index are too cool in this region compared with the others; otherwise, this phase interval is ideal. Unfortunately, there are too few points and the radii are too close in value for the algebraic method to work effectively. The temperatures show the largest discrepancy in region (1), with the values from the $B-V$ and $J-K$ indices differing by over 300 K at phase 0.15. If we define a temperature change $\Delta T_{\rm eff}$ for an index by

$$\Delta T_{\rm eff} = T_{\rm eff}(\phi = 0.15) - T_{\rm eff}(\phi = 0.55)\,, \qquad (14)$$

we can see that the optical colors show the largest changes, since values of $\Delta T_{\rm eff}$ of 928, 808, and 727 K are obtained for the $B-V$, $b-y$, and $V-R_C$ indices, respectively, compared with the results of 684 and 598 K for the $V-K$ and $J-K$ colors. Furthermore, there is a progression in these values such that the largest values are calculated from the bluest colors. These varying $\Delta T_{\rm eff}$ values cause the resulting $\theta_{\rm phot}$ amplitudes to vary as well, as shown best in Figure 7. There is also a small

TABLE 13

X ARI EFFECTIVE TEMPERATURES AND GRAVITIES

		COLOR INDEX				
PHASE	log $g_{\rm eff}$	$B-V$	$b-y$	$V-R_C$	$V-K$	$J-K$
0.15.....	2.60	6857	6645	6660	6614	6545
0.20.....	2.56	6671	6446	6471	6422	6447
0.25.....	2.58	6490	6284	6334	6292	6371
0.30.....	2.54	6331	6147	6202	6182	6285
0.35.....	2.53	6194	6050	6104	6090	6207
0.40.....	2.59	6069	5983	6025	6021	6134
0.45.....	2.56	5977	5906	5956	5960	6060
0.50.....	2.55	5944	5862	5935	5925	5988
0.55.....	2.61	5929	5837	5933	5930	5947
0.60.....	2.69	5932	5838	5952	5940	5949
0.65.....	2.74	5953	5861	5969	5983	5999
0.70.....	2.86	6049	5937	6006	6068	6109

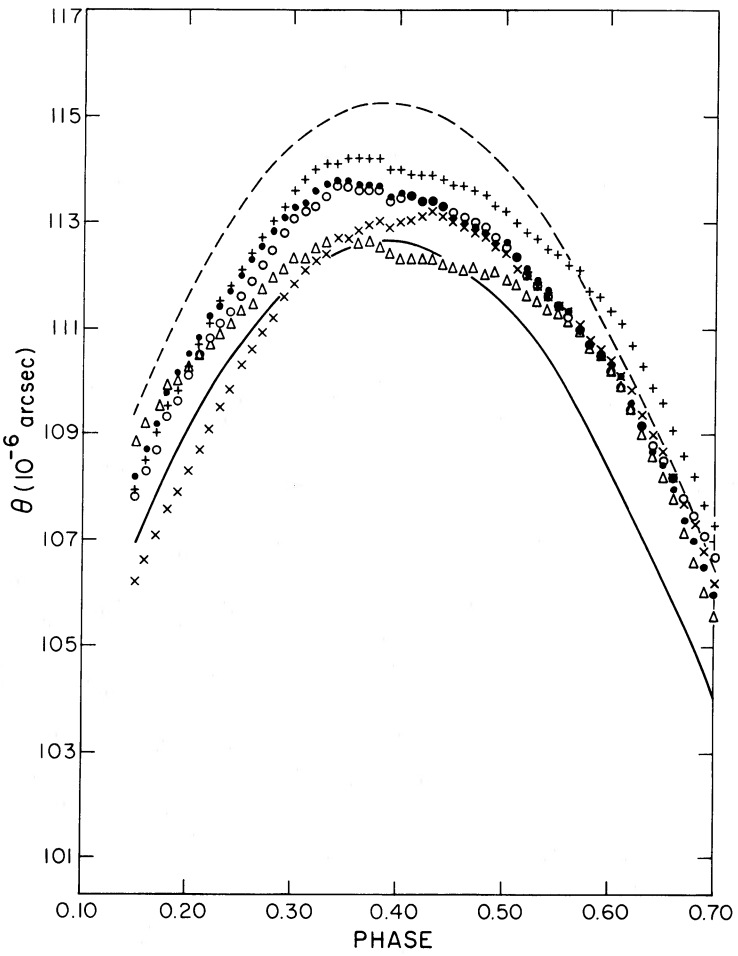

FIG. 8.—Same as Fig. 7, except that the K magnitude, rather than the V magnitude, was used to compute the "photometric diameters"

discrepancy in the temperatures of region 3. This is the phase region where the secondary "bump" in the V light curve occurs (Fig. 1; see also Figs 2–5). This "bump," which is probably due to the passage of a secondary or early shock wave (Christy 1966; Hill 1972), has a definite effect on the calculated values of θ_{phot} in this region. This effect is most pronounced in the results from the combinations of the V magnitudes with the $B-V$ and $V-R_C$ indices; however, all θ_{phot} values, with the exception of those from the $J-K$ index, are too large, as can be seen in Figures 7 and 8.

It is clear that the phasing problems of the optical colors exist because of the difference in the T_{eff} values calculated from these indices as compared with the standard temperatures from the $V-K$ index. But what is causing this difference in derived T_{eff}? The culprit or culprits seem to lurk among three possibilities: (1) incorrect estimate of $E(B-V)$, (2) incorrect values of synthetic colors for a given T_{eff}, log g_{eff}, due to incorrect model atmospheres, or (3) incorrect application of synthetic colors that are valid for static stars to a pulsating, and hence nonstatic, star.

Possibility 1 was tested by increasing the value of $E(B-V)$ by 0.05 mag. Table 14, column (4), gives the results from the algebraic method using two of the indices. The values obtained from the V, $b-y$ combination show a slight improvement in phasing; however, this is offset by a slight worsening in the phasing agreement for V, $V-K$. A decrease in $E(B-V)$ causes an increase in the asymmetry of all combinations. Possibility 2 may result from errors in either the zero point or the slopes of the color-temperature conversions. However, an arbitrary increase of 100 K in the zero point of the color-temperature conversions results in even more asymmetry in the $V-K$ values without significantly improving the $b-y$ results as shown in Table 14, column (5), while a decrease of 100 K increases the asymmetry of all results. It is possible that there is an error in the zero point of the transformation of the $b-y$ index to T_{eff}, since the values derived from this index are much lower than those from the other colors; however, this may or may not be a problem with the model atmospheres. Possibility

TABLE 14

ALGEBRAIC RESULTS FOR X ARI WITH ARBITRARY INCREASES IN $E(B-V)$, T_{eff}

			$\langle M_V \rangle$ (mag)	
MAGNITUDE	COLOR	INTERVAL	$E(B-V)+0.05$	$T_{eff}+100$ K
V	$V-K$	$0.15 \le \phi \le 0.40$	0.68	0.71
		$0.15 \le \phi \le 0.60$	0.63	0.61
V	$b-y$	$0.15 \le \phi \le 0.40$	1.40	1.61
		$0.15 \le \phi \le 0.60$	1.86	2.08
K	$b-y$	$0.15 \le \phi \le 0.40$	0.83	0.94
		$0.15 \le \phi \le 0.60$	0.98	1.06

2 was also checked by calculating the values of $T_{\rm eff}$ for Procyon, Fomalhaut, α Oph, γ Gem, and β Leo from their published colors (Johnson *et al.* 1966 for $B-V$; Hauck and Mermilliod 1979 for $b-y$; Blackwell, Shallis, and Selby 1979 and Koornneef 1983 for $V-K$ and $J-K$) and comparing them with the values of Code *et al.* (1976). There is no evidence of a systematic variation of the effective temperatures derived from these indices as compared with each other or with that of Code *et al.* (1976). However, these stars are either dwarfs or subgiants, and thus have higher surface gravities than do the RR Lyrae stars, and they also possess near-solar metallicities. Thus, the possibility that the model atmospheres are in error for metal-poor giants cannot be excluded. This can be partly resolved by investigating a metal-rich variable; but it would be desirable to have accurate temperatures for metal-poor giants in this temperature region in order to test the models adequately.

This leaves us with possibility 3. According to Castor (1966, 1972), the dynamical RR Lyrae atmsophere is in a state of "quasi-static equilibrium" throughout most of the pulsational cycle and emits a continuous spectrum almost indistinguishable from a static model at the same temperature and effective gravity. However, if the model atmospheres are indeed correct, then something is distorting the color indices, particularly the optical values. Since the problem seems to lie in phase regions 1 and 3, and not in region 2, where the star is at minimum temperature, then it is probably not due to convection, but instead may be a result of the shock waves that affect these phase regions. In order to confirm the small effect of convection on the phasing problem, the analysis of VY Ser of CL was repeated, using the $\alpha = 2$ models of Kurucz (1979) instead of the $\alpha = 1$ models. The phasing problem remained unchanged because all $\theta_{\rm phot}$ values derived from the $V, b-y$ combination were smaller by about the same amount, $2\overset{d}{.}3 \times 10^{-6}$, than the results of CL.

We cannot completely rule out either possibility 2 or possibility 3, since the cause of the different $\Delta T_{\rm eff}$ values may lie with either the slope of the color-temperature conversions of the model atmospheres or with the shock-wave phenomena. Although these differences in $T_{\rm eff}$ remain unexplained, the values from the $V-K$ index are probably valid because this index is measured over a longer baseline in wavelength. Our confidence in the infrared results is further strengthened by the absence of any phasing problems. The use of the K magnitude in the calculations yields better results because the variation in this magnitude is influenced more by the radius variation than the temperature change, and thus is less sensitive than the optical filters to temperature effects, either convective or shock-induced. We recommend the use of the $V-K$ index and the K magnitude in Baade-Wesselink calculations until the problems with the other indices can be resolved.

IV. DISCUSSION

We now analyze the sources of uncertainty in $\langle M_V \rangle$ as derived from the K, $V-K$ combination. The major source is obviously the color-temperature transformation. An error of 100 K in the zero-point causes a noticeable worsening of the results, introducing a slight phasing problem. Since it is unlikely that the zero-point error is this large, the error due to this effect is probably no more than 0.10 mag. It is possible that there is an error in the slope of the color-temperature conversion; however, this does not seem to affect the $V-K$ results.

Another source of error is the value of $E(B-V)$. Since the values of Lub (1977) and Burstein and Heiles (1978) are in good agreement, the error in $E(B-V)$ is probably no more than 0.01 mag, yielding an error in $\langle M_V \rangle$ of ± 0.05 mag. This is confirmed by the fact that the phasing problem increases if $E(B-V)$ is changed significantly. The only other major source of error is in the estimate of the pulsational velocity correction factor, p. Estimates ranging from 1.30 to 1.41 have been used in the past, although it is unlikely that p exceeds 1.35. An error of ± 0.05 in p leads to an uncertainty in the average absolute magnitude of ± 0.08 mag (Siegel 1980).

Minor sources of error include the uncertainty in the computed value of the systemic velocity. Since a velocity gradient of no more than 2 km s^{-1} may still be present, we will adopt an uncertainty in $\langle M_V \rangle$ of ± 0.05 mag due to this. Another source of error could be the metallicity. However, the analysis was also performed using colors derived for a value of [M/H] $= -1.7$, and the results for the $V-K$ index were the same as the results for the adopted metallicity of -2.2. Random errors in the photometry and the spectroscopy average out during the analysis, so this is no problem.

In conclusion, by adding the above individual errors in quandrature, we find that the final error in the average absolute magnitude is unlikely to be greater than 0.15 mag. Hence, we adopt a final value of $\langle M_V \rangle = +0.88 \pm 0.15$ mag for X Ari, which corresponds to a distance modulus of 8.23 ± 0.15 mag, or a distance of 440 ± 30 pc. This value is fainter than that derived by other investigators; however, it must be pointed out that our analysis has employed near-simultaneous photometric and spectroscopic observations. Manduca *et al.* (1981) obtained a value of $\langle M_V \rangle = 0.59 \pm 0.25$ mag for X Ari, but, since they used the radial velocity curve of Oke (1966), any phasing problem was masked by the need to apply phase shifts to correct for an uncertain ephemeris and a secularly increasing period. Oke (1966) derived $\langle M_V \rangle = +0.8 \pm 0.4$ mag, but, since he used $E(B-V) = 0.19$ mag, $p = 1.41$, $\gamma = -34$ km s^{-1}, and more primitive model atmospheres, the agreement of his results and ours is probably coincidental. The work of Siegel (1980, 1982), McNamara and Feltz (1977), and Wallerstein and Brugel (1979) also suffers from the use of radial velocity curves that are 15–20 years old and not simultaneous with the photometry. McDonald (1977) and Woolley and Savage (1971) used a mean radial velocity curve, which biases the results in such a way that the stars appear to have a similar radii. All of these investigations employed optical color indices, so each could have a hidden phasing problem, especially those using $b-y$ or $B-V$.

The only other applications of the Baade-Wesselink method that make use of simultaneous photometry and spectroscopy are those of Longmore *et al.* (1985) and Burki and Meylan (1986*a*, *b*). Both groups defined simple relationships between log $T_{\rm eff}$ and the color index in order to set up an equation that could be solved by least squares. Longmore *et al.* assumed a linear transformation between log $T_{\rm eff}$ and color, while Burki and Meylan assumed that log $T_{\rm eff}$ was a quadratic function of the color. Although it is perhaps more appropriate to use a conversion based on a linear relationship between the color and $\theta_{\rm eff}$ ($\equiv 5040$ K$/T_{\rm eff}$) rather than these transformations, this should be a minor point considering the limited range of $T_{\rm eff}$ involved. All of these transformations neglect the effects of gravity, but both groups restricted the phase interval to those phases where the effective gravity is essentially constant, so this should not be a problem. Longmore *et al.* (1985) derived a value of $\langle M_V \rangle = +0.63 \pm 0.12$ mag for VY Ser by performing

a weighted averaging of the values of the mean radius derived using the techniques of Balona (1977) upon various magnitude-color combinations, obtaining $\langle R \rangle = 6.13 \pm 0.14$ solar units in the phase interval $0.10 \leq \phi \leq 0.75$. However, as can be seen in their Table 3, the values of $\langle R \rangle$ obtained from the different combinations vary widely. The V filter yields results of 6.80 ± 0.19 and 5.50 ± 0.09 solar units when used in conjunction with the $V-J$ and the $V-K$ indices, while the results of the K filter are 5.67 ± 0.07 and 5.45 ± 0.08 solar units for these two colors. It should be more appropriate to consider only the values from the $V-K$ index. If $\langle R \rangle$ is taken to be the value obtained from the K, $V-K$ combination, then the calculated value of $\langle M_V \rangle$ becomes $+0.87$ mag, assuming that everything else is equal. It is difficult to determine whether these discrepancies in the computed mean radii are due to the method employed or to the star, since any phasing problem that may exist is hidden in the statistical analysis. Burki and Meylan (1986*a*, *b*) obtained values of $\langle M_V \rangle$ of $+0.28$ mag for RR Cet and $+0.49$ mag for DX Del by combining the results of two different methods. First of all, they assumed a log $T_{\rm eff}$–Geneva $[B-V]$ relationship that is quadratic in the color, based on the work of Burki and Benz (1982), to set up an equation solvable by nonlinear least squares, while their second method was a linear least-squares solution that employs $T_{\rm eff}$ values calculated from the model atmospheres of Grenon (1978, 1979). However, since they used an optical color index, it is difficult to judge how reliable these answers are, particularly since both methods are statistical ones that mask any possible phasing problems. Also, it is not clear from Burki and Benz (1982) why the transformation must be quadratic, since their results are sensitive to the choice of the mean radius. Furthermore, the application of the second method, the linear least-squares technique, yielded linear correlation coefficients of 0.69 for RR Cet and 0.62 for DX Del, which seem to be rather low. As a check, we applied this method to X Ari, considering different phase intervals as before to search for phasing problems. The results are presented in Table 15. Although the results for the interval $0.15 \leq \phi \leq 0.60$ using the K magnitude and the different color indices are consistent with each other and with the adopted value, there is a problem with the other values, perhaps the result of not having enough values to compute the least-squares coefficients accurately. This method seems to be less reliable than either the algebraic method or the surface brightness method, since even the $V-K$ results are significantly different in different phase intervals, so it becomes difficult to identify phasing problems.

TABLE 15

LINEAR LEAST-SQUARES RESULTS FOR X ARI[a]

		$\langle M_V \rangle$ (mag)	
MAGNITUDE	COLOR	$0.15 \leq \phi \leq 0.40$	$0.15 \leq \phi \leq 0.60$
V	$V-K$	1.25	0.84
K	$V-K$	1.25	0.84
V	$b-y$	2.42	1.54
K	$b-y$	1.48	0.92
V	$V-R_C$	1.99	1.52
K	$V-R_C$	1.35	0.91

[a] Following the method of Burki and Meylan 1986*a*.

One of the main disputes about the brightness of RR Lyrae variables is to what degree their luminosities depend upon their metallicities. The statistical parallax results of Heck and Lakaye (1978) and Clube and Dawe (1978) suggest that the metal-rich variables are much brighter than the metal-poor ones, perhaps more than half a magnitude. This is in contrast to the theoretical predictions of Christy (1966), to the relation derived by Sandage (Sandage, Katem, and Sandage 1981; Sandage 1982), and perhaps to the Baade-Wesselink results (Manduca *et al.* 1981), which maintain that the metal-poor variables should be brighter. Finally, the study of variables with widely different metallicity values in the globular cluster ω Cen by Butler, Dickens, and Epps (1978) seems to indicate no dependence of $\langle M_V \rangle$ on metallicity. Hawley *et al.* (1986) and Strugnell, Reid, and Murray (1986) used a statistical parallax analysis based on the principle of maximum likelihood to reach a similar conclusion, and found the values $\langle M_V \rangle = +0.76 \pm 0.14$ mag and $\langle M_V \rangle = +0.75 \pm 0.2$ mag, respectively. The value obtained for X Ari is consistent with these results, but more stars need to be observed before any conclusion can be drawn.

V. CONCLUSIONS

It is clear from the previous discussion that the value of the luminosity of RR Lyrae variables is still open to dispute. The Baade-Wesselink method should be able to yield results accurate to perhaps ± 0.1 mag, provided that an infrared color index such as the $V-K$ index is used to determine the values of $T_{\rm eff}$ and $m_{\rm bol}$. We plan to apply this type of analysis to field stars of widely different metallicities in order to determine the dependence of $\langle M_V \rangle$ on [M/H], if such a dependence exists. Also, we can test the period-luminosity-amplitude relation of Sandage (1981*a*, *b*; 1982) and Sandage, Katem, and Sandage (1981). An investigation into RRc type (first overtone) variables will also be undertaken to see whether the phasing problems also appear in these stars with higher temperatures and differing dynamical photospheric states.

We also plan to extend this investigation to variables in globular clusters. There are two advantages to analyzing cluster variables instead of field RR Lyrae variables: (1) because all the variables in a given cluster are at essentially the same distance, an analysis of stars of varying $\langle T_{\rm eff} \rangle$ (i.e., period) and fundamental versus first-overtone pulsators will allow us to test the physics of the phasing problem and its possible causes; (2), assuming that it all works, we should be able to measure the distance to a cluster to within 10% or better by combining the results of several variables. The observed turnoff luminosity should then give ages to a similar accuracy, an obviously important cosmological result. Further, the luminosity of the horizontal branch can be used to estimate the helium abundance, which is also significant. If our results apply to other field variables, their distances diminish. If the results also apply to globular clusters, their derived ages will increase because the inferred turnoff luminosities will be lower.

We thank Jim Crowson and Skip Schwartz for obtaining a large portion of the radial velocity data. We also wish to thank M. Siegel for the unpublished *uvbyβ* data of X Ari and other variables. This work is a partial fulfillment of the Ph.D degree requirements for R. Jones, and has been supported by NSF grant AST-8312849 to the University of North Carolina.

REFERENCES

Balona, L. A. 1977, *M.N.R.A.S.*, **178**, 231.
Blackwell, D. E., Shallis, M. J., and Selby, M. J. 1979, *M.N.R.A.S.*, **188**, 847.
Burki, G., and Benz, W. 1982, *Astr. Ap.*, **115**, 30.
Burki, G., and Meylan, G. 1986*a*, *Astr. Ap.*, **156**, 131.
———. 1986*b*, *Astr. Ap.*, **159**, 255.
Burstein, D., and Heiles, C. 1978, *Ap. J.*, **225**, 40.
Butler, D. 1975, *Ap. J.*, **200**, 68.
Butler, D., Dickens, R. J., and Epps, E. 1978, *Ap. J.*, **225**, 148.
Carney, B. W. 1980, *Ap. J. Suppl.*, **42**, 481.
Carney, B. W., and Latham, D. W. 1984, *Ap. J.*, **278**, 241 (CL).
Castor, J. I. 1966, Ph.D. thesis, California Institute of Technology.
———. 1972, in *The Evolution of Population II Stars*, ed. A. G. Davis Philip (*Dudley Obs. Rept.*, No. 4), p. 147.
Chaffee, F. H. Jr., and Peters, J. R. 1983, *A Pictorial Atlas of the Emission Line Spectrum of a Thorium-Argon Hollow Cathode Lamp* (Tucson: F. L. Whipple Observatory).
Christy, R. F. 1966, *Ap. J.*, **144**, 108.
Clube, S. V. M., and Dawe, J. A. 1978, in *IAU Symposium 80, The HR Diagram*, ed. A. G. Davis Philip and D. S. Hayes (Dordrecht: Reidel), p. 53.
———. 1980, *M.N.R.A.S.*, **190**, 591.
Code, A. D., Davis, J., Bless, R. C., and Hanbury Brown, R. 1976, *Ap. J.*, **203**, 417.
Crawford, D., and Barnes, J. V. 1970, *A.J.*, **75**, 978.
Elias, J. H., Frogel, J. A., Hyland, A. R., and Jones, T. J. 1983, *A.J.*, **88**, 1027.
Elias, J. H., Frogel, J. A., Matthews, K., and Neugebauer, G. 1982, *A.J.*, **87**, 1029.
Graham, J. A. 1973, in *IAU Colloquium 21, Variable Stars in Globular Clusters and in Related Systems*, ed. J. D. Fernie (Dordrecht: Reidel), p. 120.
———. 1975, *Pub. A.S.P.*, **87**, 641.
———. 1977, *Pub. A.S.P.*, **89**, 425.
Grenon, M. 1978, *Pub. Obs. Genève*, B, No. 5.
———. 1979, in *Problems of Calibration of Multicolor Photometric Systems*, ed. A. G. Davis Philip (*Dudley Obs. Rept.*, No. 14), p. 471.
Griersmith, D., Hyland, A. R., and Jones, T. J. 1982, *A.J.*, **87**, 1106.
Grønbech, B., Olsen, E. H., and Strömgren, B. 1976, *Astr. Ap. Suppl.*, **26**, 155.
Hauck, B., and Mermilliod, M. 1979, *uvbyβ Photoelectric Photometric Catalog* (Strasbourg: Centre de Données Stellaires).
Hawley, S. L., Jefferys, W. H., Barnes, T. G., III, and Lai, Wan. 1986, *Ap. J.*, **302**, 626.
Heck, A., and Lakaye, J. M. 1978, *M.N.R.A.S.*, **184**, 17.
Hemenway, M. K. 1975, *A.J.*, **80**, 199.
Hill, S. J. 1972, *Ap. J.*, **178**, 793.
Johnson, H. L., Mitchell, R. I., Iriarte, B., and Wiśniewski, W. Z. 1966, *Comm. Lunar Planet. Lab.*, **4**, 99.
Jones, T. J., and Hyland, A. R. 1983, *M.N.R.A.S.*, **192**, 359.
Koornneef, J. 1983, *Astr. Ap. Suppl.*, **51**, 489.
Kraft, R. P. 1982, preprint (invited talk given during Joint Discussion VII at XVIIIth General Assembly of the IAU).
Kraft, R. P., Suntzeff, N. B., Langer, G. E., Carbon, D. F., Trefzger, C. F., Friel, E., and Stone, R. P. 1982, *Pub. A.S.P.*, **94**, 55.
Kurucz, R. L. 1979, *Ap. J. Suppl.*, **40**, 1.
Landolt, A. U. 1983, *A.J.*, **88**, 439.
Latham, D. W. 1985, in *IAU Colloquium 88, Stellar Radial Velocities*, ed. A. G. Davis Philip and D. W. Latham (Schenectady: Davis), p. 21.
Longmore, A. J., Fernley, J. A., Jameson, R. F., Sherrington, M. R., and Frank, J. 1985, *M.N.R.A.S.*, **216**, 873.
Lub, J. 1977, Ph.D. thesis, University of Leiden.
Manduca, A., and Bell, R. A. 1981, *Ap. J.*, **250**, 306.
Manduca, A., Bell, R. A., Barnes, T. G., III, Moffett, T. J., and Evans, D. S. 1981, *Ap. J.*, **250**, 312.
McDonald, L. H. 1977, Ph.D. thesis, University of California at Santa Cruz.
McNamara, D. H., and Feltz, K. A., Jr. 1977, *Pub. A.S.P.*, **89**, 699.
Moore, C. E., Minnaert, M. G. J., and Houtgast, J. 1966, *The Solar Spectrum, 2935 Å to 8770 Å* (NBS Monog., No. 61).
Oke, J. B. 1966, *Ap. J.*, **145**, 468.
Oke, J. B., Giver, L. P., and Searle, L. 1962, *Ap. J.*, **136**, 393 (OGS).
Oort, J. H., and Plaut, L. 1975, *Astr. Ap.*, **41**, 71.
Philip, A. G. D., and Philip, K. D. 1973, *Ap. J.*, **179**, 855.
Preston, G. W., and Paczyński, B. 1964, *Ap. J.*, **140**, 181.
Sandage, A. 1970, *Ap. J.*, **162**, 841.
———. 1981*a*, *Ap. J. (Letters)*, **244**, L23.
———. 1981*b*, *Ap. J.*, **248**, 161.
———. 1982, *Ap. J.*, **252**, 553.
Sandage, A., Katem, B., and Sandage, M. 1981, *Ap. J. Suppl.*, **46**, 41.
Sanford, R. F. 1949, *Ap. J.*, **109**, 208.
Siegel, M. J. 1980, M.S. thesis, University of Maryland.
———. 1981, private communication.
———. 1982, *Pub. A.S.P.*, **94**, 122.
Strugnell, P., Reid, N., and Murray, C. A. 1986, *M.N.R.A.S.*, **220**, 413.
Sturch, C. 1966, *Ap. J.*, **143**, 774.
Thompson, W. J. 1984, *Computing in Applied Science* (New York: Wiley), pp. 55–58, 248.
van den Bergh, S., and Pritchet, C. J. 1986, paper presented at 167th meeting of the AAS.
Wallerstein, G., and Brugel, E. W. 1979, *A.J.*, **84**, 1840.
Wesselink, A. J. 1969, *M.N.R.A.S.*, **144**, 297.
Woolley, R., and Dean, J. 1976, *M.N.R.A.S.*, **177**, 247.
Woolley, R., and Savage, A. 1971, *Royal Obs. Bull.*, **170**, 365.
Wyatt, W. F., 1985, in *IAU Colloquium 88, Stellar Radial Velocities*, ed. A. G. Davis Philip and D. W. Latham (Schenectady: Davis), p. 123.
Zessewitch, W. P., Firmaniuk, B. N., and Kreiner, J. M. 1982, *Rocznik Astr. Obs. Kracow*, No. 54.

BRUCE W. CARNEY and RODNEY V. JONES: Department of Physics and Astronomy, Phillips Hall 039A, University of North Carolina, Chapel Hill, NC 27514

ROBERT L. KURUCZ and DAVID W. LATHAM: Harvard-Smithsonian Center for Astrophysics, 60 Garden Street, Cambridge, MA 02138